Received: 17 January 2024 | Revised: 19 April 2024 | Accepted: 23 May 2024

DOI: 10.1002/num.23120

RESEARCH ARTICLE

WILEY

An efficient flux-variable approximation scheme for Darcy's flow

Rajan B. Adhikari[1] | **Imbumn Kim**[2] | **Young Ju Lee**[3] | **Dongwoo Sheen**[2]

[1]Department of Mathematics, Oklahoma State University, Stillwater, Oklahoma, USA
[2]Department of Mathematics, Seoul National University, Seoul, Korea
[3]Department of Mathematics, Texas State University, San Marcos, Texas, USA

Correspondence
Dongwoo Sheen, Department of Mathematics, Seoul National University, Seoul 08826, Korea.
Email: sheen@snu.ac.kr

Funding information
National Science Foundation, Grant/Award Numbers: DMS 2208289, DMS 1318465, DMS 2208499; National Research Foundation of Korea, Grant/Award Numbers: 2017R1A2B3012506, 2015M3C4A7065662.

Abstract

We present an efficient numerical method to approximate the flux variable for the Darcy flow model. An important feature of our new method is that the approximate solution for the flux variable is obtained without approximating the pressure at all. To accomplish this, we introduce a user-defined parameter delta, which is typically chosen to be small so that it minimizes the negative effect resulting from the absence of the pressure, such as inaccuracy in both the flux approximation and the mass conservation. The resulting algebraic system is of significantly smaller degrees of freedom, compared to the one from the mixed finite element methods or least-squares methods. We also interpret the proposed method as a single step iterate of the augmented Lagrangian Uzawa applied to solve the mixed finite element in a special setting. Lastly, the pressure recovery from the flux variable is discussed and an optimal-order error estimate for the method is obtained. Several examples are provided to verify the proposed theory and algorithm, some of which are from more realistic models such as SPE10.

KEYWORDS

Darcy's flow, finite element method, flux variable, hybrid method

1 | INTRODUCTION

Let Ω be a bounded open domain in $\mathbb{R}^d, d = 2, 3$, with boundary $\Gamma = \overline{\Gamma}_N \cup \overline{\Gamma}_D$. We are interested in solving the following equation for $\mathbf{u}$ and p:

$$\mathbf{u} = -\frac{\mathbb{K}}{\mu}\nabla p \quad \text{in } \Omega, \tag{1.1a}$$

$$\nabla \cdot \mathbf{u} = f \quad \text{in } \Omega, \tag{1.1b}$$

$$\mathbf{u} \cdot \boldsymbol{\nu} = g \quad \text{on } \Gamma_N, \tag{1.1c}$$

$$p = g_D \quad \text{on } \Gamma_D, \tag{1.1d}$$

where $\boldsymbol{\nu}$ denotes the unit outward normal vector to the boundary Γ, $\mathbb{K}$ and μ are the permeability tensor of the medium and the viscosity of the fluid, respectively, and f, g and g_D are the volumetric flow rate source or sink, the prescribed normal flux and pressure on the boundary, respectively. The Equation (1.1) arises in the single phase flows in porous media, Ω, governed by the Darcy flow model:

$$\mathbf{u} = -\frac{\mathbb{K}}{\mu}(\nabla \tilde{p} + \rho \mathbf{g}), \quad \text{and} \quad \nabla \cdot \mathbf{u} = f,$$

subject to the boundary conditions:

$$\mathbf{u} \cdot \boldsymbol{\nu} = g, \quad \text{on } \Gamma_N \quad \text{and} \quad \tilde{p} = \tilde{g}_D, \quad \text{on } \Gamma_D,$$

where ρ represents the density of the fluid, $\mathbf{g}$ is the gravity vector, $\tilde{g}_D$ is a modification of g_D obtained by interchanging between $\tilde{p}$ and p, and $\mathbf{u}$ and $\tilde{p}$ are the Darcy flow rate and the pressure in the fluid. Note that the modified pressure given in (1.1) can be obtained through $p = \tilde{p} + \rho g_c z$, where g_c and z are the gravity scalar and the coordinate of gravitational direction, respectively.

The difficulty in the practical simulation of Darcy flow model arises from the irregularities of the domain boundaries Γ_D and Γ_N and the permeability tensor $\mathbb{K}$. We shall assume that Ω is Lipschitz and its boundary parts Γ_D and Γ_N satisfy some regularity condition that will be specified later. We shall only assume that $\mathbb{K} \in \mathbb{R}^{d\times d}$ is a $d \times d$ bounded, symmetric and uniformly positive definite matrix and $\mu \in L^\infty(\Omega)$.

We shall attempt to solve the Equation (1.1) using the finite element methods. For the sake of presentation of finite element methods, we shall use standard Sobolev spaces. For example, for region K in $\mathbb{R}^d$, let $(\cdot,\cdot)_K$, $\langle\cdot,\cdot\rangle_{\partial K}$, $\|\cdot\|_{0,K}$, and $|\cdot|_{0,\partial K}$ denote the $L^2(K)$ and $L^2(\partial K)$ inner products and norms, respectively, and so on. In case $K = \Omega$, the subindex may be omitted and furthermore the index 0 may be dropped, too. We set the following Sobolev space:

$$\mathbf{V} = \mathbf{H}_{\Gamma_N,0}(\text{div}; \Omega) = \{\mathbf{v} \in \mathbf{H}(\text{div}; \Omega) \mid \boldsymbol{\nu} \cdot \mathbf{v} = 0 \text{ on } \Gamma_N\}, \tag{1.2}$$

and $W = L^2(\Omega)$. For the sake of simplicity in notations, we shall denote the norm on $\mathbf{H}(\text{div}; \Omega)$ as $\|\cdot\|_V$ and the norm on L^2 as $\|\cdot\|_W$ or simply $\|\cdot\|$, respectively. The symbol $\|\cdot,\cdot\|_{V\times W}$ denotes the product norm for the product space $\mathbf{V} \times W$.

Throughout this article, for the sake of simplicity, we shall assume that $g = 0$ on Γ_N for the Equation (1.1). If it is not the case, we can introduce $\mathbf{u}_0 \in \mathbf{H}(\text{div}; \Omega)$ such that $\mathbf{u}_0 \cdot \boldsymbol{\nu} = g$ and write the Equation (1.1) in terms of $\tilde{\mathbf{u}} = \mathbf{u} - \mathbf{u}_0$. This shall result in the modified right hand sides for (1.1a) and (1.1b). Note that this modification does not change p or its boundary condition g_D. We also further

assume that $\Gamma_D \neq \emptyset$. This is because the case $\Gamma_D = \emptyset$ leads us to discuss some additional constraints for the well-posedness of the problem. More precisely, if the Neumann condition is prescribed in the entire boundary, Γ, that is, $\Gamma_N = \Gamma$, then the compatibility condition must be given as follows:

$$\int_\Omega f dx = \int_\Gamma g \, ds, \tag{1.3}$$

for a unique existence of solution $p \in H^1(\Omega)/\mathbb{R}$. Lastly, we shall use a standard Sobolev space notation, that is, $L^a(\Omega)$ with $1 \leq a \leq \infty$ denotes the space of functions whose a^{th} power is integrable over the domain Ω and $W^{k,a}(\Omega)$ for $1 \leq a \leq \infty$ denotes the space of functions in $L^a(\Omega)$ whose first k derivatives are in L^a space. Now for $f \in L^2(\Omega)$, the standard mixed weak formulation of (1.1) is to find $(\mathbf{u}, p) \in \mathbf{H}_{\Gamma_N,0}(\text{div}; \Omega) \times L^2(\Omega)$ such that

$$(\mathbb{A}\mathbf{u}, \mathbf{v}) - (p, \nabla \cdot \mathbf{v}) = -\langle g_D, \boldsymbol{\nu} \cdot \mathbf{v} \rangle_{\Gamma_D}, \quad \forall\, \mathbf{v} \in \mathbf{H}_{\Gamma_N,0}(\text{div}; \Omega), \tag{1.4a}$$

$$(\nabla \cdot \mathbf{u}, q) = (f, q), \quad \forall\, q \in L^2(\Omega), \tag{1.4b}$$

where $\mathbb{A} = \left(\frac{\mathbb{K}}{\mu}\right)^{-1}$. We note that the system (1.4) can be cast into the following operator form to find $(\mathbf{u}, p) \in \mathbf{H}_{\Gamma_N,0}(\text{div}; \Omega) \times L^2(\Omega)$ such that for $G \in \mathbf{H}_{\Gamma_N,0}(\text{div}; \Omega)'$ and $F \in L^2(\Omega)$,

$$\begin{pmatrix} \mathcal{A} & \mathcal{B}^* \\ \mathcal{B} & 0 \end{pmatrix} \begin{pmatrix} \mathbf{u} \\ p \end{pmatrix} = \begin{pmatrix} G \\ F \end{pmatrix}, \tag{1.5}$$

where $\mathcal{A} : \mathbf{H}(\text{div}; \Omega) \mapsto \mathbf{H}_{\Gamma_N,0}(\text{div}; \Omega)'$, $\mathcal{B} := \nabla\cdot : \mathbf{H}(\text{div}; \Omega) \mapsto L^2(\Omega)$ and $\mathcal{B}^*$ is its adjoint operator of $\mathcal{B}$.

Our error analysis in Theorem 4 exploits the regularity estimate of weak solution of the Laplace operator with mixed boundary conditions. For non-smooth domains, while the estimate for a Dirichlet or a Neumann boundary condition is well-known, much less has been done for a mixed boundary condition. For this reason, we will make the following regularity assumptions on Γ. We let that Γ_D has a positive measure, and that Γ_N satisfies the following conditions with $B = B(0; 1)$ denoting the unit ball in $\mathbb{R}^d$:

1. there exists a family $(U_0, U_1, \ldots, U_J)$ of open sets of $\mathbb{R}^d$ such that
$$\overline{\Omega} \subset \cup_{j=0}^k U_j, \ \overline{U_0} \subset \Omega;$$
2. there exists a corresponding family of functions $(\phi_1, \ldots, \phi_J)$ such that $\phi_j : U_j \to B$ is one-to-one and ϕ_j and ϕ_j^{-1} are Lipschitz-continuous fulfilling one of the following conditions:
   a. $U_j \cap \Gamma_N = U_j \cap \Gamma$ and ϕ_j satisfies
   $$\phi_j(U_j \cap \Omega) = B \cap \mathbb{R}^d_+(\text{ with } x_d > 0) := B_+, \tag{1.6a}$$
   $$\phi_j(U_j \cap \Gamma) = B \cap \mathbb{R}^{d-1}(\text{ with } x_d = 0) := B^{d-1}; \tag{1.6b}$$
   b. $U_j \cap \Gamma_N = \emptyset$ and ϕ_j satisfies (1.6a);
   c. $$\begin{cases} \phi_j(U_j \cap \Omega) = \{x \in B \mid x_d > 0, x_{d-1} > 0\} =: B_{++}, \\ \phi_j(U_j \cap \Gamma_D) = \{x \in B \mid x_d = 0, x_{d-1} > 0\}, \\ \phi_j(U_j \cap \Gamma_N) = \{x \in B \mid x_d > 0, x_{d-1} = 0\}. \end{cases}$$

We use the notation $W^{k,a}_{\Gamma_D,0}(\Omega)$ to represent the set of functions in $W^{k,a}(\Omega)$ whose trace on Γ_D is zero, and use the shorthand $H^k(\Omega)$ for $W^{k,2}(\Omega)$. The dual spaces of $H^1_{\Gamma_D,0}(\Omega)$ and $W^{1,a}_{\Gamma_D,0}(\Omega)$ are denoted

by $H^{-1}_{\Gamma_D}(\Omega)$ and $W^{-1,a}_{\Gamma_D}(\Omega)$, respectively. Additionally, we define

$$2^* = \begin{cases} \frac{2d}{d-2} & \text{if } d > 2, \\ \infty & \text{if } d \leq 2, \end{cases} \text{ that is, } 2^* = \begin{cases} 6 & \text{if } d = 3, \\ \infty & \text{if } d \leq 2. \end{cases}$$

The following theorem, which corresponds to Theorem 4 in [14], is included here for completeness.

Theorem 1. *There exists ℓ_0 with $2 < \ell_0 \leq 2^*$ such that whenever $p \in H^1_{\Gamma_D,0}(\Omega)$ is a weak solution of*

$$(\mathbb{A}\nabla p, \nabla q) = \langle f, q\rangle_{W^{-1,\ell}_{\Gamma_D}(\Omega),\ H^1_{\Gamma_D,0}(\Omega)} \quad \forall\ q \in H^1_{\Gamma_D,0}(\Omega) \tag{1.7}$$

for some $2 \leq \ell < \ell_0$ and $f \in W^{-1,\ell}_{\Gamma_D}(\Omega)$, then $p \in W^{1,\ell}_{\Gamma_D,0}(\Omega)$ and

$$\|p\|_{W^{1,\ell}_{\Gamma_D,0}(\Omega)} \leq C(\ell)\|f\|_{W^{-1,\ell}_{\Gamma_D}(\Omega)}. \tag{1.8}$$

For smooth domains, the following stronger result is found to be established by using the notion of fractional order Sobolev spaces:

$$\|p\|_{H^{1+s}_{\Gamma_D,0}(\Omega)} \leq C\|f\|_{H^{-1+s}_{\Gamma_D}(\Omega)}, \text{ for some } s > 0. \tag{1.9}$$

We refer our readers to (e.g., [6, 31]) for the estimate (1.9) and to (e.g., [12]) for the fractional order Sobolev spaces.

The standard technique to solve the system (1.4) is the mixed finite element method. We point out that the mixed finite element is in general difficult to formulate since it requires certain cares to adopt a suitable stable pair of finite element spaces for $\mathbf{u}$ and p, as well as to design a fast solver. Our motivation in this article is that typical application areas of fluid mechanics such as subsurface flow modeling, do not require calculations of pressure while accurate and efficient approximations of flux is crucial. Namely, the use of standard mixed finite element methods devoted to approximate both flux and pressure as accurate as possible simultaneously by distributing computational efforts to the approximation of both flux and pressure variables can be overkill in practice. In this spirit, we have introduced a new *light* scheme to compute the flux variable, that is, a parameter-dependent hybrid two-step method in our prior work [24]. In this scheme, a pressure is approximated very roughly in a very coarse mesh by using a standard Galerkin scheme, or its variant; then, a parameter-dependent $H(\text{div})$-variational form with appropriate right hand side is set and solved in a finer mesh. This technique is shown to give an optimal order flux approximation.

In the current paper, we improve the hybrid two-step method, [24]. That is, we show that the $H(\text{div})$-variational form is the only equation needed to be solved, that is, the first step to obtain rough approximate pressure can be skipped to obtain the desired flux variable of optimal accuracy. This shall therefore lead us to obtain a single-step method. The advantage of the proposed approach is that the bilinear equation is $H(\text{div})$-elliptic, and it is free from the restriction of discrete inf-sup condition, since it employs only the $H(\text{div})$ vector part of mixed finite element space pairs for which there have been several efficient preconditioners for $H(\text{div})$-bilinear form equation, just to cite a few, [3, 4, 16, 18, 19, 22]. Additionally, we provide a new interpretation of the single step flux approximation as a single step iterate of augmented Lagrangian Uzawa applied to solve the mixed finite element in a special setting. Lastly, although it is not our primary interest to approximate the pressure variable accurately, we provide a scheme to compute the pressure based on the flux approximation as well.

The rest of our article is organized as follows. In Section 2, preliminaries results concerning the mixed finite element methods for second order elliptic equations with mixed boundary conditions are presented. A single step flux approximate scheme is then presented in Section 3 and error estimates

are provided in Section 4. Confirming numerical results for the theoretical development are presented in Section 5.

2 | PRELIMINARIES ON THE MIXED FINITE ELEMENT METHOD AND THE HYBRID TWO-STEP METHOD

In this section, we review the classical mixed finite element spaces, but point out some recent result as presented in [26] that is needed to understand and solve the mixed finite element for second order elliptic equations with mixed boundary conditions (1.4).

2.1 | Mixed finite element method for second order elliptic problem

To obtain approximate solutions for (1.4), let $\mathcal{T}_h$ be a family of shape regular triangulation of Ω, where $h = \max_{K\in\mathcal{T}_h} h_K, h_K = \mathrm{diam}(K)$, see [9]. First, we briefly review some of the properties of the classical mixed finite element spaces. Denote by $\mathbb{RT}_h^{(k)}$ and $\mathbb{BDM}_h^{(k)}$ the Raviart–Thomas–Nédélec space [27, 29] and the Brezzi-Douglas-Marini or Brezzi-Douglas-Duran-Fortin space of index $k \geq 1$ [10, 11] defined as follows:

$$\begin{cases} \mathbb{RT}_h^{(k)} := \{\mathbf{v} \in \mathbf{H}(\mathrm{div};\,\Omega) \;:\; \mathbf{v}|_K \in [P_k(K)]^d \oplus \mathrm{Span}\{\mathbf{x}\widetilde{P}_k(K)\},\ K \in \mathcal{T}_h\}, \\ \mathbb{BDM}_h^{(k)} := \{\mathbf{v} \in \mathbf{H}(\mathrm{div};\,\Omega) \;:\; \mathbf{v}|_K \in [P_k(K)]^d, \quad K \in \mathcal{T}_h\}, \end{cases}$$

where $P_k(K)$ denotes the space of all polynomials up to degree k defined on K, and $\widetilde{P}_k(K)$ the space of all homogeneous polynomials of degree k. Denote by $C^0(P_h^{(k)})$ the standard C^0-conforming finite element spaces of piecewise polynomials of degree $\leq k$ on mesh $\mathcal{T}_h$. By $C^{-1}(P_h^{(k)})$ we also designate the space of piecewise polynomials of degree $\leq k$ on mesh $\mathcal{T}_h$, namely, $C^{-1}(P_h^{(k)}) = \{q \in L^2(\Omega) \;:\; q|_K \in P_k(K),\ K \in \mathcal{T}_h\}$. We set

$$\mathbb{RT}_{0,h}^{(k)} = \mathbb{RT}_h^{(k)} \cap \mathbf{H}_{\Gamma_N,0}(\mathrm{div};\,\Omega), \quad \mathbb{BDM}_{0,h}^{(k)} = \mathbb{BDM}_h^{(k)} \cap \mathbf{H}_{\Gamma_N,0}(\mathrm{div};\,\Omega).$$

Next, we define the family of RTN/BDM-BDDF mixed finite element spaces of index $k, k = 0, 1, \ldots$, by

$$\mathbb{M}_{0,h}^{(k)} := \mathbf{V}_{0,h}^{(k)} \times W_h^{(k)} := \begin{cases} \mathbb{RT}_{0,h}^{\iota(k)} \times C^{-1}(P_h^{(k)}), \\ \mathbb{BDM}_{0,h}^{\iota(k)} \times C^{-1}(P_h^{(k)}), \end{cases}$$

where

$$\iota(k) = \begin{cases} k, & \text{if } \mathbf{V}_{0,h}^{(k)} = \mathbb{RT}_{0,h}^{\iota(k)}, \\ k+1, & \text{if } \mathbf{V}_{0,h}^{(k)} = \mathbb{BDM}_{0,h}^{\iota(k)}. \end{cases}$$

Denote by $\mathbb{N}_{0,h}^{(k)}$ the space $C^0(P_h^{(k+1)}) \cap H^1_{\Gamma_N}(\Omega)$ in 2D and the Nédélec element of degree k as a subspace of $\mathbf{H}_0(\mathrm{curl};\,\Omega)$ in 3D, respectively: that is,

$$\mathbb{N}_{0,h}^{(k)} := \{\mathbf{v} \in \mathbf{H}_{\Gamma_N,0}(\mathrm{curl};\Omega) \;:\; \mathbf{v}|_K \in [P_k(K)]^3 \oplus \mathrm{Span}\{\mathbf{q} \in [\widetilde{P}_{k+1}(K)]^3 \;:\; \mathbf{x}\cdot\mathbf{q} = 0,\ K \in \mathcal{T}_h\}.$$

The key to prove the well-posedness of the above mixed formulation (1.4) and other related finite element theory is at the (partial) de Rham complex [2, 5, 8, 17] (in two and three space dimensions) with mixed boundary conditions with the bounded interpolation operator. This has been established in

[26], which can be stated as follows:

$$\begin{array}{ccccc} \mathbf{H}_{\Gamma_N,0}(\mathrm{curl};\Omega) & \xrightarrow{\mathrm{curl}} & \mathbf{H}_{\Gamma_N,0}(\mathrm{div};\Omega) & \xrightarrow{\mathrm{div}} & L^2(\Omega) \\ \downarrow \Pi_h^{\mathrm{curl}} & & \downarrow \Pi_h^{\mathrm{div}} & & \downarrow \Pi_h^0 \\ \mathbb{N}_{0,h}^{(k)} & \xrightarrow{\mathrm{curl}} & \mathbf{V}_{0,h}^{(k)} & \xrightarrow{\mathrm{div}} & W_{0,h}^{(k)} \end{array} \tag{2.1}$$

Namely, we have that

$$\nabla \cdot \Pi_h^{\mathrm{div}} \mathbf{u} = \Pi_h^0 \nabla \cdot \mathbf{u}, \quad \forall \mathbf{u} \in \mathbf{H}_{\Gamma_N,0}(\mathrm{div};\Omega). \tag{2.2}$$

Let ∇_h be the discrete gradient operator $\nabla_h : W_{0,h}^{(k)} \to \mathbf{V}_{0,h}^{(k)}$ or the adjoint operator with respect to L^2 inner product, defined as follows: for $q_h \in W_{0,h}^{(k)}$,

$$(\nabla_h q_h, \mathbf{v}_h) = -(q_h, \nabla \cdot \mathbf{v}_h), \quad \forall \mathbf{v}_h \in \mathbf{V}_{0,h}^{(k)}. \tag{2.3}$$

Then, we have the (discrete) Helmholtz decomposition via the closed range theory (see also [3], [20, Lemmas 2.5 and 2.6]), that is,

$$\mathbf{V}_{0,h}^{(k)} = \nabla \times \mathbb{N}_{0,h}^{(k)} \oplus \nabla_h W_{0,h}^{(k)} = \mathcal{N}(\mathrm{div}) \oplus \mathcal{R}(\mathrm{div}^*). \tag{2.4}$$

Note that the orthogonality holds both in $L^2(\Omega)$ and in $\mathbf{H}(\mathrm{div};\Omega)$ inner product.

The mixed finite element approximation for (1.4) is then to find $(\mathbf{u}_h^M, p_h^M) \in \mathbf{V}_{0,h}^{(k)} \times W_{0,h}^{(k)}$ such that

$$(\mathbb{A}\mathbf{u}_h^M, \mathbf{v}_h) - (p_h^M, \nabla \cdot \mathbf{v}_h) = -\langle g_D, \boldsymbol{\nu} \cdot \mathbf{v}_h \rangle_{\Gamma_D}, \quad \forall\ \mathbf{v}_h \in \mathbf{V}_{0,h}^{(k)}, \tag{2.5a}$$

$$(\nabla \cdot \mathbf{u}_h^M, q_h) = (f, q_h), \quad \forall\ q_h \in W_{0,h}^{(k)}. \tag{2.5b}$$

For fixed k and boundary conditions, we shall simply put $\mathbf{V}_h := \mathbf{V}_{0,h}^{(k)}$ and $W_h := W_{0,h}^{(k)}$ for simplicity. In deriving error estimates, we will take advantage of the well-known mixed finite element method error estimates: we refer the reader to [7, 10, 11, 13, 15, 23] and references therein.

Theorem 2. *The Equation (2.5) produces the approximate solution* $(\mathbf{u}_h^M, p_h^M) \in \mathbf{V}_h \times W_h$ *to Darcy law (1.1) such that the following error estimates hold true*:

$$\|(\mathbf{u} - \mathbf{u}_h, p - p_h)\|_{V \times W} \lesssim \inf_{\mathbf{v}_h, q_h \in \mathbf{V}_h \times W_h} \|(\mathbf{u} - \mathbf{v}_h, p - q_h)\|_{V \times W}. \tag{2.6}$$

Proof. We note that it is standard to show that the Darcy law is well-posed. On the other hand, this is true as well that

$$(\mathbb{A}\mathbf{v}_h, \mathbf{v}_h) \gtrsim \|\mathbf{v}_h\|_V^2, \quad \forall \mathbf{v}_h \in \mathbf{Z}_h = \{\mathbf{v}_h \in \mathbf{V}_h : b(\mathbf{v}, \psi) = 0, \quad \forall \psi \in W_h\}. \tag{2.7}$$

From the de Rham complex, we have that

$$b(\mathbf{v} - \Pi_h^{\mathrm{div}} \mathbf{v}, \psi) = 0, \quad \forall \mathbf{v} \in \mathbf{V}_h, \psi \in W_h. \tag{2.8}$$

Furthermore, it holds that Π_h^{div} is stable. Namely, it is a Fortin operator. This establishes the discrete inf-sup condition. The quasi-optimality is then standard. This completes the proof. ∎

2.2 | The hybrid two-step approximations

In this section, we shall review the hybrid two-step method introduced in [24]. We shall begin with a simple but important lemma:

Algorithm 1. Hybrid two-step scheme [24]

For a fixed $\ell \geq 1$ and $\delta>0$, we perform:Find $p_H^G \in C^0(P_H^{(\ell)})$ such that

$$(\mathbb{A}^{-1}\nabla p_H^G, \nabla q_H) = (f, q_H), \quad \forall\, q_H \in C^0(P_H^{(\ell)}). \tag{2.13}$$

Use p_H^G to find $\mathbf{u}_h \in \mathbf{V}_h$ such that

$$(\nabla\cdot\mathbf{u}_h, \nabla\cdot\mathbf{v}_h) + \delta(\mathbb{A}\mathbf{u}_h, \mathbf{v}_h) = (f + \delta p_H^G, \nabla\cdot\mathbf{v}_h) - \delta\,\langle g_D, \boldsymbol{\nu}\cdot\mathbf{v}_h\rangle_{\Gamma_D}, \quad \forall \mathbf{v}_h \in \mathbf{V}_h. \tag{2.14}$$

Lemma 1. *Let $\delta > 0$ be a parameter and $(\mathbf{u}, p)$ be the solution of mixed weak form (1.4). Assume that $\mathbf{u}^\delta \in \mathbf{H}_{\Gamma_N,0}(\mathrm{div};\,\Omega)$ solves*

$$(\nabla\cdot\mathbf{u}^\delta, \nabla\cdot\mathbf{v}) + \delta(\mathbb{A}\mathbf{u}^\delta, \mathbf{v}) = (f + \delta p, \nabla\cdot\mathbf{v}) - \delta\langle g_D, \boldsymbol{\nu}\cdot\mathbf{v}\rangle_{\Gamma_D}, \quad \forall \mathbf{v} \in \mathbf{H}_{\Gamma_N,0}(\mathrm{div};\,\Omega). \tag{2.9}$$

Then $\mathbf{u} = \mathbf{u}^\delta$ for all $\delta > 0$.

Proof. Take $q = \nabla\cdot\mathbf{v}$ in (1.4b) to get

$$(\nabla\cdot\mathbf{u}, \nabla\cdot\mathbf{v}) = (f, \nabla\cdot\mathbf{v}), \quad \forall\, \mathbf{v} \in \mathbf{H}_{\Gamma_N,0}(\mathrm{div};\,\Omega), \tag{2.10}$$

which is then added to (1.4a) multiplied by δ to obtain

$$(\nabla\cdot\mathbf{u}, \nabla\cdot\mathbf{v}) + \delta(\mathbb{A}\mathbf{u}, \mathbf{v}) = (f + \delta p, \nabla\cdot\mathbf{v}) - \delta\langle g_D, \boldsymbol{\nu}\cdot\mathbf{v}\rangle_{\Gamma_D}, \quad \forall\, \mathbf{v} \in \mathbf{H}_{\Gamma_N,0}(\mathrm{div};\,\Omega). \tag{2.11}$$

We now subtract (2.11) from (2.9) to we have

$$(\nabla\cdot(\mathbf{u}^\delta - \mathbf{u}), \nabla\cdot\mathbf{v}) + \delta(\mathbb{A}(\mathbf{u}^\delta - \mathbf{u}), \mathbf{v}) = 0, \quad \forall\, \mathbf{v} \in \mathbf{H}_{\Gamma_N,0}(\mathrm{div};\,\Omega). \tag{2.12}$$

Therefore, by choosing $\mathbf{v} = \mathbf{u} - \mathbf{u}^\delta$ in (2.12), we arrive at $\mathbf{u}^\delta = \mathbf{u}$ if $\delta > 0$. This completes the proof. ∎

The two-step hybrid method obtains the approximation of pressure and then obtain the flux by solving (2.9) as described as in Algorithm 1. Recall that the two step solvers rely on two meshes, which is allowed to be independent, one for approximating the primary variable, and the other for flux variable and such an independent nature is compensated for by an appropriate choice of the parameter δ to arrive at an optimal accuracy of the flux variable via an appropriate transfer of the primary variable for the discrete equation of (2.9). We also note that the problem (2.14) can be understood as solving a bilinear form equation: find $\mathbf{u}_h \in \mathbf{V}_h$ such that

$$\Lambda_h(\mathbf{u}_h, \mathbf{v}_h) = (f + \delta p_H^G, \nabla\cdot\mathbf{v}_h) - \delta\langle g_D, \boldsymbol{\nu}\cdot\mathbf{v}_h\rangle_{\Gamma_D}, \quad \mathbf{v}_h \in \mathbf{V}_h, \tag{2.15}$$

where $\Lambda_h(\mathbf{u}_h, \mathbf{v}_h) = (\nabla\cdot\mathbf{u}_h, \nabla\cdot\mathbf{v}_h) + \delta(\mathbb{A}\mathbf{u}_h, \mathbf{v}_h)$. For an appropriate solution technique for Λ_h, we refer to works by Arnold et al. [3, 4] and also Hiptmair and Xu in [19].

3 | SIMPLE PARAMETER-DEPENDENT APPROXIMATION OF FLUX VARIABLE AND PRESSURE RECOVERY

It was shown that in [24], the Algorithm 1 can obtain an optimally accurate flux approximation using an approximate solution p_H^G for p on a coarse mesh of size H if δ is appropriately chosen. In this section, we shall show that it is really not necessary to construct an approximate solution p_H^G at all. Thus, in order

Algorithm 2. Single step scheme for flux approximation

For a fixed $\delta>0$, we perform:Find $\mathbf{u}_h \in \mathbf{V}_h$ such that

$$(\nabla\cdot\mathbf{u}_h, \nabla\cdot\mathbf{v}_h) + \delta(\mathbb{A}\mathbf{u}_h, \mathbf{v}_h) = (f, \nabla\cdot\mathbf{v}_h) - \delta\,\langle g_D, \boldsymbol{\nu}\cdot\mathbf{v}_h\rangle_{\Gamma_D}, \quad \forall \mathbf{v}_h \in \mathbf{V}_h. \tag{3.1}$$

Algorithm 3. Pressure recovery Scheme 1

Given $\mathbf{u}_h \in \mathbf{V}_h$, find $p_h \in W_h$ such that

$$(p_h, \nabla\cdot\mathbf{v}_h) = (\mathbb{A}\mathbf{u}_h, \mathbf{v}_h) + \langle g_D, \boldsymbol{\nu}\cdot\mathbf{v}_h\rangle_{\Gamma_D}, \quad \forall\, \mathbf{v}_h \in \mathbf{V}_h. \tag{3.2}$$

to obtain a good flux approximation $\mathbf{u}_h$, it is unnecessary to consider two hybrid grids, but we may take into account a finer grid only. Furthermore, we shall interpret both the hybrid two step method and the newly proposed single step method in a unified framework. This is based on an insight on how to interpret the parameter-dependent flux approximation. In fact, we show that the parameter-dependent flux approximation can be viewed as a single step iterative solution via augmented Lagrangian Uzawa applied to the mixed finite element formulation. On a separate issue, although it is not our primary interest to approximate the primary variable p, it can be approximated from the flux $\mathbf{u}_h$ as indicated in (2.5). We provide two algorithms to recover the pressure approximation as accurate as the one from the standard mixed finite element method.

3.1 | The single step flux approximation

We shall begin with a simple scheme for the approximation of the flux variable $\mathbf{u}$ in (1.1). We drop the term $\delta(p_H^G, \nabla\cdot\mathbf{v}_h)$ in (2.14) and propose a new simpler scheme Algorithm 2 to approximate $\mathbf{u}$ by $\mathbf{u}_h \in \mathbf{V}_h$. We then propose the Algorithm 3 below to recover an accurate pressure approximation $p_h \in W_h$ from the flux $\mathbf{u}_h$ obtained in Algorithm 2. It is easy to observe that the unique existence of $\mathbf{u}_h$ solving(3.1) and p_h solving (3.2) follows directly from the Lax-Milgram lemma and the discrete de Rham sequence (2.1), respectively.

Before passing to the next subsection, we observe that the following error equation can be obtained immediately from (1.4) and (3.1):

$$(\nabla\cdot(\mathbf{u}-\mathbf{u}_h), \nabla\cdot\mathbf{v}_h) + \delta(\mathbb{A}(\mathbf{u}-\mathbf{u}_h), \mathbf{v}_h) = \delta(p, \nabla\cdot\mathbf{v}_h), \quad \forall \mathbf{v}_h \in \mathbf{V}_h, \tag{3.3}$$

where $(\mathbf{u}, p) \in \mathbf{H}_{\Gamma_N,0}(\mathrm{div};\Omega)\times L^2(\Omega)$ and $\mathbf{u}_h \in \mathbf{V}_h$ are the solutions satisfying (1.4) and (3.1), respectively. The equation will be useful in our error analysis to follow.

3.2 | The single-step and hybrid two-step methods and the augmented Lagrangian Uzawa method

In this section, we shall provide a view of both the proposed single step and hybrid two-step method for flux approximation, as a single step iterate of the augmented Lagrangian Uzawa method for the mixed method. This view provides an alternative way to recover the pressure from the flux as well. We begin our discussion by casting the mixed finite element formulation (2.5) as the operator equation to

Algorithm 4. Augmented Lagrangian Uzawa iterative method [25]

Set $\ell = 0$ and for a given $p^{\ell} \in W_h$ and we perform:Find $\mathbf{u}^{\ell+1}$ by solving the following equation:

$$\left(\mathcal{A}_h + \frac{1}{\delta}\mathcal{B}_h^*\mathcal{B}_h\right)\mathbf{u}^{\ell+1} + \mathcal{B}_h^* p^{\ell} = G_h + \frac{1}{\delta}\mathcal{B}_h^* F_h. \tag{3.6}$$

Update the pressure to obtain $p^{\ell+1}$ as follows:

$$p^{\ell+1} = p^{\ell} + \frac{1}{\delta}(F_h - \mathcal{B}_h\mathbf{u}^{\ell+1}). \tag{3.7}$$

Go to Step 1 if $(\mathbf{u}^{\ell+1}, p^{\ell+1})$ is not a desired solution pair.

find $(\mathbf{u}_h^M, p_h^M) \in \mathbf{V}_h \times W_h$ as follows:

$$\begin{pmatrix} \mathcal{A}_h\mathcal{B}_h^* \\ \mathcal{B}_h 0 \end{pmatrix}\begin{pmatrix} \mathbf{u}_h^M \\ p_h^M \end{pmatrix} = \begin{pmatrix} G_h \\ F_h \end{pmatrix}, \tag{3.4}$$

where $\mathcal{A}_h, \mathcal{B}_h, \mathcal{B}_h^*$, G_h and F_h are discrete version of $\mathcal{A}, \mathcal{B}, \mathcal{B}^*, G$ and F. The augmented Lagrangian Uzawa begins with the stabilization by $\mathcal{B}_h^*\mathcal{B}_h$ of the above equation as follows:

$$\begin{pmatrix} \mathcal{A}_h + \frac{1}{\delta}\mathcal{B}_h^*\mathcal{B}_h\mathcal{B}_h^* \\ \mathcal{B}_h 0 \end{pmatrix}\begin{pmatrix} \mathbf{u}_h^M \\ p_h^M \end{pmatrix} = \begin{pmatrix} G_h + \frac{1}{\delta}\mathcal{B}_h^* F_h \\ F_h \end{pmatrix}. \tag{3.5}$$

The augmented Lagrangian Uzawa iterative method applied for the mixed formulation (3.5) can then read as follows: given an approximate pressure p_H^G, the flux approximation $\mathbf{u}_h^{\delta} = \mathbf{u}_h$, the solution to the system (2.14) can be shown to satisfy the following equation in an operator form:

$$\left(\mathcal{A}_h + \frac{1}{\delta}\mathcal{B}_h^*\mathcal{B}_h\right)\mathbf{u}_h + \mathcal{B}_h^* Q_h^W p_H^G = \frac{1}{\delta}\mathcal{B}_h^* Q_h^W F_h + G_h, \tag{3.8}$$

where Q_h^W is the L^2 projection onto the space W_h. Equivalently, we have the following formulae for $\mathbf{u}_h$ given as follows:

$$\mathbf{u}_h = \left(\mathcal{A}_h + \frac{1}{\delta}\mathcal{B}_h^*\mathcal{B}_h\right)^{-1}\left(\frac{1}{\delta}\mathcal{B}_h^* Q_h^W F_h + G_h - \mathcal{B}_h^* Q_h^W p_H^G\right). \tag{3.9}$$

This is exactly the single iterate from the augmented Lagrangian Uzawa method introduced in Algorithm 4. We further note that the reference solution $\overline{\mathbf{u}}_h$ defined with exact pressure p, is given as follows:

$$\overline{\mathbf{u}}_h = \left(\mathcal{A}_h + \frac{1}{\delta}\mathcal{B}_h^*\mathcal{B}_h\right)^{-1}\left(\frac{1}{\delta}\mathcal{B}_h^* Q_h^W F_h + G_h - \mathcal{B}_h^* Q_h^W p\right). \tag{3.10}$$

Set $\mathbf{e}_u = \mathbf{u}_h - \overline{\mathbf{u}}_h$ and $\mathbf{e}_p = p_H^G - p$. Then the error equation is given as follows:

$$\mathbf{e}_u = \mathbf{u}_h - \overline{\mathbf{u}}_h = \left(\mathcal{A}_h + \frac{1}{\delta}\mathcal{B}_h^*\mathcal{B}_h\right)^{-1}\left(-\mathcal{B}_h^* Q_h^W \mathbf{e}_p\right).$$

This means that

$$\begin{aligned}(\mathcal{A}_h\mathbf{e}_u, \mathbf{e}_u) &= \left(\mathcal{A}_h\left(\mathcal{A}_h + \frac{1}{\delta}\mathcal{B}_h^*\mathcal{B}_h\right)^{-1}\mathcal{B}_h^* Q_h^W \mathbf{e}_p, \left(\mathcal{A}_h + \frac{1}{\delta}\mathcal{B}_h^*\mathcal{B}_h\right)^{-1}\mathcal{B}_h^* Q_h^W \mathbf{e}_p\right) \\ &\leq \left(\mathcal{B}_h^* Q_h^W \mathbf{e}_p, \left(\mathcal{A}_h + \frac{1}{\delta}\mathcal{B}_h^*\mathcal{B}_h\right)^{-1}\mathcal{B}_h^* Q_h^W \mathbf{e}_p\right) \\ &= \left(Q_h^W \mathbf{e}_p, \left[\mathcal{B}_h\left(\mathcal{A}_h + \frac{1}{\delta}\mathcal{B}_h^*\mathcal{B}_h\right)^{-1}\mathcal{B}_h^*\right] Q_h^W \mathbf{e}_p\right) \leq \delta\|Q_h^W \mathbf{e}_p\|^2 \leq \delta\|\mathbf{e}_p\|^2.\end{aligned}$$

To summarize, we have proved the following estimate:

$$\|\mathbf{e}_u\|_{\mathbb{A}} \leq \sqrt{\delta}\|\mathbf{e}_p\| \quad \text{or equivalently} \quad \|\mathbf{u}_h - \overline{\mathbf{u}}_h\|_{\mathbb{A}} \leq \sqrt{\delta}\|p_H^G - p\|.$$

This indicates that even if we choose $p_H^G = 0$, we are able to obtain good approximation for sufficiently small choice of δ. More precise error analysis can be found at Section 4 below. Our conclusion is that both the single step and hybrid two-step method can be viewed as a single step iterate of the augmented Lagrangian Uzawa method. Recently, this observation has led to a couple of applications for designing the constrained optimization in image processings [21, 28]. In particular, this view is used to obtain an alternative pressure recovery from the flux $\mathbf{u}_h$ (see Algorithm 5 below).

Algorithm 5. Pressure recovery Scheme 2

Given $\mathbf{u}_h \in \mathbf{V}_h$, we set $p^\ell = Q_h^W p_H^G$, $\mathbf{u}^{\ell+1} = \mathbf{u}_h$Update the pressure using the following formula:

$$p_h := Q_h^W p_H^G + \frac{1}{\delta}(F_h - \mathcal{B}_h \mathbf{u}_h). \tag{3.11}$$

Then we notice that a standard argument can lead to the following error estimate for the pressure update given in Equation (3.11)

$$\|p_h^M - p_h\| \leq \frac{1}{(1 + \mu_0 \frac{1}{\delta})}\|p_h^M - p_H^G\|, \tag{3.12}$$

where μ_0 is the minimum eigenvalue for the Schur complement operator for the discrete mixed finite element system (3.4), that is, $\mathbb{S} = \mathcal{B}_h \mathcal{A}_h^{-1} \mathcal{B}_h^*$. While the augmented Lagrangian Uzawa has been used extensively, the choice of the parameter δ has not been paid too much attention. Our theoretical contribution is at the optimal choice of this parameter δ in terms of accuracy.

4 | ERROR ANALYSIS AND CHOICES OF δ

In this section, we provide error estimates for our approximate solution $\mathbf{u}_h$ in both L^2 and $\mathbf{H}(\mathrm{div}; \Omega)$ norms. The corresponding error analysis for p_h, the pressure recovery, shall also be presented. Our estimates shall shed light on the choice of the problem parameter $\delta > 0$ to achieve optimal-order rates of convergence. The error analysis performed in this section in relation with the parameter δ shall guide how the augmented Lagrangian Uzawa method chooses an optional parameter to achieve an accurate solution in a single iteration as well.

4.1 | Error analysis to $\mathbf{u}_h$ and $\nabla \cdot \mathbf{u}_h$

We begin with the investigation of convergence behavior of $\mathbf{u}_h$, the approximate solution to $\mathbf{u}$ obtained by Algorithm 2. We use the weighted L^2 norm $\|\mathbf{v}\|_{\mathbb{A}}^2 = (\mathbb{A}\mathbf{v}, \mathbf{v})$ to simplify the notation. Here and in what follows, C represents a generic positive constant independent of the mesh size h.

Theorem 3. *Assume that the solution* $\mathbf{u}$ *of (1.4) belongs to* $H^s(\Omega)$. *Let* $\mathbf{u}_h \in \mathbf{V}_h^{(k)}$ *be the solution satisfying (3.1). Then,*

$$\|\mathbf{u}_h - \mathbf{u}\|_{\mathbb{A}} \leq C\left[h^s\|\mathbf{u}\|_s + \sqrt{\delta}\|p\|\right], \quad s \leq \iota(k) + 1. \tag{4.1}$$

Furthermore, if $\nabla \cdot \mathbf{u}$ *of Problem (1.4) belongs to* $H^s(\Omega)$, *we have*

$$\|\nabla \cdot (\mathbf{u}_h - \mathbf{u})\| \leq C\big[h^s \|\nabla \cdot \mathbf{u}\|_s + \delta \|p\|\big], \quad s \leq k+1. \tag{4.2}$$

Proof. Let $(\mathbf{u}_h^M, p_h^M) \in \mathbb{M}_h^{(k)}$ be the mixed finite element solution satisfying (2.5). For a fixed $\mathbf{v}_h \in \mathbf{V}_h^{(k)}$, by multiplying (2.5a) by δ, setting $q_h = \nabla \cdot \mathbf{v}_h$ in (2.5b), and adding the resulting terms, we obtain

$$(\nabla \cdot \mathbf{u}_h^M, \nabla \cdot \mathbf{v}_h) + \delta(\mathbb{A}\mathbf{u}_h^M, \mathbf{v}_h) = (f + \delta\, p_h^M, \nabla \cdot \mathbf{v}_h) - \delta\langle g_D, \boldsymbol{\nu} \cdot \mathbf{v}_h\rangle_{\Gamma_D}. \tag{4.3}$$

Now, by subtracting (3.1) from (4.3), we get

$$\big(\nabla \cdot (\mathbf{u}_h^M - \mathbf{u}_h), \nabla \cdot \mathbf{v}_h\big) + \delta\big(\mathbb{A}(\mathbf{u}_h^M - \mathbf{u}_h), \mathbf{v}_h\big) = \delta\big(p_h^M, \nabla \cdot \mathbf{v}_h\big). \tag{4.4}$$

In particular, we choose $\mathbf{v}_h = \mathbf{u}_h^M - \mathbf{u}_h$ to obtain

$$\|\nabla \cdot (\mathbf{u}_h^M - \mathbf{u}_h)\|^2 + \delta \|\mathbf{u}_h^M - \mathbf{u}_h\|_{\mathbb{A}}^2 \leq \delta \|p_h^M\| \|\nabla \cdot (\mathbf{u}_h^M - \mathbf{u}_h)\|.$$

First of all, this results in

$$\|\nabla \cdot (\mathbf{u}_h^M - \mathbf{u}_h)\| \leq \delta \|p_h^M\|, \tag{4.5}$$

which in turns gives

$$\|\mathbf{u}_h^M - \mathbf{u}_h\|_{\mathbb{A}} \leq \sqrt{\delta}\|p_h^M\|. \tag{4.6}$$

We now recall the error estimates for the mixed finite element method [7, 10, 11, 29]:

$$\|p_h^M - p\| \leq C\, h^s \|p\|_s \quad \text{for } s \leq \iota(k)+1, \tag{4.7a}$$

$$\|\mathbf{u}_h^M - \mathbf{u}\|_{\mathbb{A}} \leq C\, h^s \|\mathbf{u}\|_s \quad \text{for } s \leq \iota(k)+1, \tag{4.7b}$$

$$\|\nabla \cdot (\mathbf{u}_h^M - \mathbf{u})\| \leq C\, h^s \|\nabla \cdot \mathbf{u}\|_s \quad \text{for } s \leq k+1. \tag{4.7c}$$

Applying the triangle inequality, and combining (4.5), (4.7b), and (4.7), we have

$$\begin{aligned}\|\mathbf{u}_h - \mathbf{u}\|_{\mathbb{A}} &\leq \|\mathbf{u} - \mathbf{u}_h^M\|_{\mathbb{A}} + \|\mathbf{u}_h^M - \mathbf{u}_h\|_{\mathbb{A}} \\ &\leq C\Big[h^s \|\mathbf{u}\|_s + \sqrt{\delta}\|p_h^M\|\Big],\end{aligned}$$

for $s \leq \iota(k)+1$. Then (4.1) follows from the last estimate combined with the following triangle inequality:

$$\|p_h^M\| \leq \|p_h^M - p\| + \|p\| \leq Ch^s \|\mathbf{u}\|_s + \|p\|. \tag{4.8}$$

Moreover, if $\nabla \cdot \mathbf{u}$ of Problem (1.4) belongs to $H^s(\Omega)$, we have

$$\begin{aligned}\|\nabla \cdot (\mathbf{u}_h - \mathbf{u})\| &\leq \|\nabla \cdot (\mathbf{u} - \mathbf{u}_h^M)\| + \|\nabla \cdot (\mathbf{u}_h^M - \mathbf{u}_h)\| \\ &\leq C\big[h^s \|\nabla \cdot \mathbf{u}\|_s + \delta \|p_h^M\|\big],\end{aligned}$$

for $s \leq k+1$. Using the triangle inequality and plugging (4.7a), the last inequality leads to (4.2). This completes the proof. ∎

Two special cases for the lowest-order RTN and BDM families are explicitly given in the following two corollaries.

Corollary 4.1. *Assume that* $\mathbf{u}$ *of Problem (1.4) belongs to* $H^1(\Omega)$ *and that* $\delta \leq C\, h^2$. *Let* $\mathbf{u}_h \in \mathbb{RT}_h^{(0)}$ *be the solution satisfying (3.1). Then,*

$$\|\mathbf{u}_h - \mathbf{u}\|_{\mathbb{A}} \leq C\, h\, (\|\mathbf{u}\|_1 + \|p\|)\,. \tag{4.9}$$

Furthermore, if $\nabla \cdot \mathbf{u}$ *of Problem (1.4) belongs to* $H^1(\Omega)$, *we have*

$$\|\nabla \cdot (\mathbf{u}_h - \mathbf{u})\| \leq C\, h\, (\|\nabla \cdot \mathbf{u}\|_1 + h\|p\|)\,. \tag{4.10}$$

Proof. Choose $k = 0, s = 1$, and $\delta = h^2$ in (4.1) to get (4.9). These choices sufficiently lead to get (4.10) from (4.2). ∎

Corollary 4.2. *Assume that* $\mathbf{u}$ *of Problem (1.4) belongs to* $H^2(\Omega)$ *and that* $\delta \leq C\, h^4$. *Let* $\mathbf{u}_h \in \mathbb{BDM}_h^{(1)}$ *be the solution satisfying (3.1). Then,*

$$\|\mathbf{u}_h - \mathbf{u}\|_{\mathbb{A}} \leq C\, h^2\, (\|\mathbf{u}\|_2 + \|p\|)\,, \tag{4.11}$$

and

$$\|\nabla \cdot (\mathbf{u}_h - \mathbf{u})\| \leq C\, h\, \left(\|\nabla \cdot \mathbf{u}\|_1 + h^3\|p\|\right). \tag{4.12}$$

Proof. Recall that $\iota(k) = k + 1$ for BDM family, and choose $k = 0, s = 2$, and $\delta = h^4$ in (4.1) to get (4.11). These choices sufficiently lead to get (4.12) from (4.2). ∎

Remark 1. For the RTN family with $k = 0$, that is, taking $\mathbb{RT}_h^{(0)}$ ($\iota(k) = 0$ in this case) as the hybrid space, let us consider solving the L-shaped domain problem. In this case, $p \in H^{1+\alpha}(\Omega)$ with $\alpha = \frac{2}{3}$ and $\nabla \cdot \mathbf{u} = 0$. In this case, $\delta = h^{\frac{4}{3}}$ is chosen for an optimal convergence rate $\mathcal{O}(h^\alpha)$, as stated in (4.1). For numerical examples, see the case of partial elliptic regularity in Section 5.2.

4.2 | Error analysis to p_h

In this section, we provide a convergence result of p_h obtained by Algorithm 3 to p, the pressure recovery.

Theorem 4. *Assume that the solution* p *of the Equation (1.4) belongs to* $H^{s+1}(\Omega)$. *Let* $p_h \in W_h$ *be the solution to (3.2). Then, we have*

$$\|p_h - p\| \leq C\left[h^s\|p\|_{s+1} + \sqrt{\delta}\|p\|\right], \quad s \leq \iota(k) + 1. \tag{4.13}$$

Furthermore, if Ω *is smooth and* $\frac{\mathbb{K}}{\mu}$ *in (1.1) is in* $C^1(\Omega)$, *then*

$$\|Q_h^W p - p_h\| \leq C\left[h^r\left(\|\mathbf{u}_h - \mathbf{u}\|_{\mathbb{A}} + \|\nabla \cdot \mathbf{u} - Q_h^W \nabla \cdot \mathbf{u}\|\right) + \delta\|p\|_{s+1}\right] \tag{4.14}$$

for some $r > 0$, *where* Q_h^W *is the local* L^2 *projection of* W *onto* W_h, $\mathbf{u}$ *is the solution of (1.4), and* $\mathbf{u}_h$ *is the solution of (3.1).*

Proof. Choose $\mathbf{v}_h \in \mathbf{V}_h$, such that $\nabla \cdot \mathbf{v}_h = p_h - Q_h^W p$ with $\|\mathbf{v}_h\| \leq C\|p_h - Q_h^W p\|$. Then, by the definition of Q_h^W, we have

$$\begin{aligned}
\|p_h - Q_h^W p\|^2 &= (p_h - Q_h^W p, \nabla \cdot \mathbf{v}_h) \\
&= (p_h - p, \nabla \cdot \mathbf{v}_h) = (\mathbb{A}(\mathbf{u}_h - \mathbf{u}), \mathbf{v}_h) \\
&\leq C\|\mathbf{u}_h - \mathbf{u}\|_{\mathbb{A}}\, \|\mathbf{v}_h\| \\
&\leq C\|\mathbf{u}_h - \mathbf{u}\|_{\mathbb{A}}\, \|p_h - Q_h^W p\|.
\end{aligned}$$

That is,

$$\|p_h - Q_h^W p\| \le C\|\mathbf{u}_h - \mathbf{u}\|_{\mathbb{A}}.$$

Now applying the triangle inequality, the last inequality, approximation property of Q_h^W, and Theorem 3, we obtain

$$\|p_h - p\| \le \|p_h - Q_h^W p\| + \|Q_h^W p - p\|, \tag{4.15}$$

$$\le \|\mathbf{u}_h - \mathbf{u}\|_{\mathbb{A}} + \|Q_h^W p - p\|, \tag{4.16}$$

$$\le C\left[h^s\|p\|_{s+1} + \sqrt{\delta}\|p_h^M\|\right], \text{ for } s \le \iota(k) + 1. \tag{4.17}$$

Then (4.13) follows from the last estimate combined with the following inequality:

$$\|p_h^M\| \le \|p_h^M - p\| + \|p\| \le Ch^s\|p\|_{s+1} + \|p\|.$$

This completes the proof of (4.13).

To prove (4.14), we consider the following dual problem

$$\begin{aligned} -\operatorname{div}(\mathbb{A}^{-1}\nabla q) &= Q_h^W p - p_h \text{ in } \Omega,\\ (\mathbb{A}^{-1}\nabla q)\cdot\boldsymbol{\nu} &= 0 \text{ on } \Gamma_N,\\ q &= 0 \text{ on } \Gamma_D. \end{aligned} \tag{4.18}$$

Let q be the weak solution of problem (4.18) of the form (1.7) and $\mathbf{w} = -\mathbb{A}^{-1}\nabla q$ in Ω. Then $\nabla\cdot\mathbf{w} = Q_h^W p - p_h$. Using the commutative property (2.2), we obtain $\nabla\cdot\Pi_h^{\text{div}}\mathbf{w} = Q_h^W\nabla\cdot\mathbf{w} = Q_h^W p - p_h$. Then

$$\begin{aligned} \|Q_h^W p - p_h\|^2 = (Q_h^W p - p_h, \nabla\cdot\Pi_h^{\text{div}}\mathbf{w}) &= (p - p_h, \nabla\cdot\Pi_h^{\text{div}}\mathbf{w})\\ &= (\mathbb{A}(\mathbf{u} - \mathbf{u}_h), \Pi_h^{\text{div}}\mathbf{w})\\ &= (\mathbb{A}(\mathbf{u} - \mathbf{u}_h), \Pi_h^{\text{div}}\mathbf{w} - \mathbf{w}) + (\mathbb{A}(\mathbf{u} - \mathbf{u}_h), \mathbf{w}). \end{aligned} \tag{4.19}$$

Using the approximation property of Π_h^{div}, the first term on the right-hand side of the last equation can be estimated as:

$$\begin{aligned} (\mathbb{A}(\mathbf{u} - \mathbf{u}_h), \Pi_h^{\text{div}}\mathbf{w} - \mathbf{w}) &\le C\|\mathbf{u} - \mathbf{u}_h\|_{\mathbb{A}}\|\Pi_h^{\text{div}}\mathbf{w} - \mathbf{w}\|\\ &\le Ch^r\|\mathbf{u} - \mathbf{u}_h\|_{\mathbb{A}}\|\|\mathbf{w}\|_r \le Ch^r\|\mathbf{u} - \mathbf{u}_h\|_{\mathbb{A}}\|\|q\|_{r+1}, \end{aligned} \tag{4.20}$$

for some $r \in (0, 1]$. To obtain an estimate of the second term, we apply integration by parts and split the term as follows:

$$\begin{aligned} (\mathbb{A}(\mathbf{u} - \mathbf{u}_h), \mathbf{w}) &= -(\mathbb{A}(\mathbf{u} - \mathbf{u}_h), \mathbb{A}^{-1}\nabla q) = -(\mathbf{u} - \mathbf{u}_h, \nabla q)\\ &= (\nabla\cdot(\mathbf{u} - \mathbf{u}_h), q)\\ &= (\nabla\cdot(\mathbf{u} - \Pi_h^{\text{div}}\mathbf{u}) + \nabla\cdot(\Pi_h^{\text{div}}\mathbf{u} - \mathbf{u}_h), q - Q_h^W q + Q_h^W q)\\ &= (\nabla\cdot\mathbf{u} - Q_h^W\nabla\cdot\mathbf{u}, q - Q_h^W q) + (Q_h^W\nabla\cdot\mathbf{u} - \nabla\cdot\mathbf{u}_h, Q_h^W q)\\ &= (\nabla\cdot\mathbf{u} - Q_h^W\nabla\cdot\mathbf{u}, q - Q_h^W q) + (\nabla\cdot(\mathbf{u} - \mathbf{u}_h), Q_h^W q). \end{aligned} \tag{4.21}$$

Then using the approximation property of Q_h^W, the first term on the right-hand side of the last equation can be estimated by:

$$(\nabla\cdot\mathbf{u} - Q_h^W\nabla\cdot\mathbf{u}, q - Q_h^W q) \le \|\nabla\cdot\mathbf{u} - Q_h^W\nabla\cdot\mathbf{u}\|\|q - Q_h^W q\| \le Ch^r\|\nabla\cdot\mathbf{u} - Q_h^W\nabla\cdot\mathbf{u}\|\|q\|_r. \tag{4.22}$$

To estimate the last term in (4.21), we first subtract (3.1) from (1.4b) with $q = \nabla \cdot \mathbf{v}_h$ and use the recovery equation (3.2) to find

$$(\nabla \cdot (\mathbf{u} - \mathbf{u}_h), \nabla \cdot \mathbf{v}_h) = \delta \left[(\mathbb{A}\mathbf{u}_h, \mathbf{v}_h) + \langle g_D, \mathbf{v}_h \cdot \boldsymbol{\nu} \rangle_{\Gamma_D} \right] = \delta (p_h, \nabla \cdot \mathbf{v}_h) \quad \forall\, \mathbf{v}_h \in \mathbf{V}_h.$$

Then choosing $\mathbf{v}_h$ such that $\nabla \cdot \mathbf{v}_h = Q_h^W q$, and applying (4.13), the last equation yields

$$\begin{aligned} (\nabla \cdot (\mathbf{u} - \mathbf{u}_h), Q_h^W q) = \delta (p_h, Q_h^W q) &\le \delta \|p_h\| \|q\| \le \delta (\|p - p_h\| + \|p\|) \|q\| \\ &\le C\delta (h^s \|p\|_{s+1} + \sqrt{\delta} \|p\|) \|q\| \\ &\le C\delta \|p\|_{s+1} \|q\|. \end{aligned} \tag{4.23}$$

The estimate for the last term in (4.19) is obtained by plugging (4.22) and (4.23) into (4.21). Then plugging (4.20) for the first term and applying the estimate provided by (1.9), one obtains (4.14). ∎

Remark 2. The local post-processing scheme proposed in [32] utilizes the mixed finite element solutions computed in $\mathbf{V}_h^{(k)} \times W_h^{(k)}$ to develop a more accurate approximation of the primary variable in the higher degree space $W_h^{(k+1)}$. Here, we present the scheme adapted to our finite element solutions to approximate the pressure p with increased accuracy and provide a result demonstrating the accuracy improvement. We denote Q_h^W by $Q_h^{(k)}$ to emphasize the polynomial degree and extend the notation to write $Q_h^{(i)}$ for the local L^2 projection of W onto $W_h^{(i)}$ for integer $i \ge 0$. Then the post-processing solution $p_h^* \in W_h^{(k+1)}$ is defined element-by-element through $p_h^*|_K \in P_{k+1}(K)$ as a solution ϕ_h of the formulation

$$(\mathbb{A}^{-1} \nabla \phi_h, \nabla q_h)_K = (f, q_h)_K - \langle \mathbf{u}_h \cdot \boldsymbol{\nu}_K, q_h \rangle_{\partial K} \quad \forall\, q_h \in (I - Q_h^{(0)}|_K) W_h^{(k+1)}|_K \tag{4.24a}$$

subject to

$$Q_h^{(0)}|_K \phi_h = Q_h^{(0)}|_K p_h, \tag{4.24b}$$

where $\boldsymbol{\nu}_K$ is the outward unit normal vector on the boundary of K. The solution p_h^* is found to achieve the following improved accuracy

$$\|p - p_h^*\| \le C \left[h \left(\|\mathbf{u} - \mathbf{u}_h\|_{\mathbb{A}} + \|\Pi_h^{\mathrm{div}} \mathbf{u} - \mathbf{u}\|_{0,h} \right) + \left\| p - Q_h^{(k+1)} p \right\|_{0,h} + \left\| Q_h^{(k)} p - p_h \right\| \right], \tag{4.25}$$

where $\|\cdot\|_{0,h}$ is the mesh-dependent norm defined by $\|q\|_{0,h}^2 = \|q\|^2 + \sum_{K \in \mathcal{T}_h} h_K^2 |q|_{1,K}^2$ for functions $q \in L^2(\Omega)$ with $q|_K \in H^1(K)\ \forall\, K \in \mathcal{T}_h$ and $\|\mathbf{v}\|_{0,h}^2 = \|\mathbf{v}\|^2 + \sum_{K \in \mathcal{T}_h} h_K \|\mathbf{v} \cdot \boldsymbol{\nu}_K\|_{0,\partial K}^2$ for functions $\mathbf{v} \in \mathbf{H}(\mathrm{div}; \Omega)$ with $\mathbf{v} \cdot \boldsymbol{\nu}_K \in L^2(\partial K)\ \forall\, K \in \mathcal{T}_h$. The above error estimate is established using the same arguments as in Theorem 2.2 in [32] and applying the trace inequality (see e.g., [1]).

5 | NUMERICAL EXAMPLES

In this section, we present sample results from numerical experiments to confirm our theoretical results as well as to demonstrate the effectivity and the robustness of our algorithm. For all the numerical examples, in order to look at convergence behaviors closely, uniform meshes are used instead of adaptive meshes. On the other hand, the small parameter δ makes the system of equations nearly singular, for which round-off errors are observed to cause accuracy deterioration. In our numerical computation, we use defect corrections to overcome round-off errors. Namely, using a solution obtained by the direct solver, we obtain a residual and calculate correction by solving the system once more. The improved accuracy of the solution is reported in our numerical tables.

TABLE 1 Errors and their reduction ratios of $\mathbf{u}_h \in \mathbb{RT}_h^{(0)}$ and p for the pressure boundary condition (5.2a); the parameter δ is chosen as h^2.

DOFs	h	$\|\mathbf{u}-\mathbf{u}_h^{h^2}\|$	Rate	$\|\mathbf{u}-\mathbf{u}_h^{h^2}\|_{\mathrm{div}}$	Rate	$\|p-p_h\|$	Rate
56	1/4	6.37378e−01	x	3.25377e+00	x	1.50786e−01	x
208	1/8	3.24488e−01	0.9740	1.63642e+00	0.9916	7.82612e−02	0.9461
800	1/16	1.63279e−01	0.9908	8.19426e−01	0.9979	3.94786e−02	0.9872
3136	1/32	8.18073e−02	0.9970	4.09866e−01	0.9995	1.97822e−02	0.9969
12,416	1/64	4.09294e−02	0.9991	2.04952e−01	0.9999	9.89644e−03	0.9992
49,408	1/128	2.04685e−02	0.9997	1.02478e−01	1.0000	4.94889e−03	0.9998

TABLE 2 Errors and their reduction ratios of $\mathbf{u}_h \in \mathbb{BDM}_h^{(1)}$ and p for the pressure boundary condition (5.2a); the parameter δ is chosen as h^4.

DOFs	h	$\|\mathbf{u}-\mathbf{u}_h^{h^4}\|$	Rate	$\|\mathbf{u}-\mathbf{u}_h^{h^4}\|_{\mathrm{div}}$	Rate	$\|p-p_h\|$	Rate
112	1/4	1.53125e−01	x	3.25371e+00	x	1.50782e−01	x
416	1/8	4.06233e−02	1.9143	1.63641e+00	0.9916	7.82634e−02	0.9461
1600	1/16	1.03491e−02	1.9728	8.19424e−01	0.9979	3.94786e−02	0.9873
6272	1/32	2.60407e−03	1.9907	4.09865e−01	0.9995	1.97822e−02	0.9969
24,832	1/64	6.74000e−04	1.9499	2.04952e−01	0.9999	9.89645e−03	0.9992

TABLE 3 Errors and their reduction ratios of $\mathbf{u}_h \in \mathbb{RT}_h^{(0)}$ and p for the flux boundary condition (5.2b); the parameter δ is chosen as h^2.

DOFs	h	$\|\mathbf{u}-\mathbf{u}_h^{h^2}\|$	Rate	$\|\mathbf{u}-\mathbf{u}_h^{h^2}\|_{\mathrm{div}}$	Rate	$\|p-p_h\|$	Rate
40	1/4	6.60495e−01	x	3.25377e+00	x	1.52770e−01	x
176	1/8	3.28211e−01	1.0089	1.63642e+00	0.9916	7.84947e−02	0.9607
736	1/16	1.63847e−01	1.0023	8.19426e−01	0.9979	3.95068e−02	0.9905
3008	1/32	8.18911e−02	1.0006	4.09866e−01	0.9995	1.97857e−02	0.9976
12,160	1/64	4.09415e−02	1.0001	2.04952e−01	0.9999	9.89688e−03	0.9994
48,896	1/128	2.04702e−02	1.0000	1.02478e−01	1.0000	4.94894e−03	0.9999

5.1 | The case of full elliptic regularity

We begin with a simple example with the identity tensor, that is, $\mathbb{A} = \mathbb{I}$, given as follows. With the domain $\Omega = (0,1)^2$, the following problem is considered:

$$\mathbf{u} = -\nabla p, \quad \text{in } \Omega, \tag{5.1a}$$

$$\nabla \cdot \mathbf{u} = f, \quad \text{in } \Omega, \tag{5.1b}$$

on the boundary Γ of which one of the following two boundary conditions are assumed:

$$p = g, \quad \text{on } \Gamma, \tag{5.2a}$$

$$\boldsymbol{\nu} \cdot \mathbf{u} = g, \quad \text{on } \Gamma. \tag{5.2b}$$

Here, f and g are generated by the analytic solution $p(x,y) = x^3y + y^4 + \sin(\pi x)\cos(\pi y)$. For this example, uniform triangulations of Ω are adopted in our numerical simulation and the approximation of the flux variable, $\mathbb{RT}_h^{(0)}$ and $\mathbb{BDM}_h^{(1)}$ spaces are employed.

Tables 1 and 2 show errors in the computation of the flux variable applying the hybrid method with pressure boundary condition (5.2a) and give optimal convergence rates in the approximation of the flux variable. The choices of parameter are set to $\delta = h^2$ for $\mathbb{RT}_{g,h}^{(0)}$ and $\delta = h^4$ for $\mathbb{BDM}_{g,h}^{(1)}$.

Also the case where the flux boundary condition (5.2b) is solved is shown in Tables 3 and 4 with parameters $\delta = h^2$ for $\mathbb{RT}_h^{(0)}$ and $\delta = h^4$ for $\mathbb{BDM}_h^{(1)}$.

TABLE 4 Errors and their reduction ratios of $\mathbf{u}_h \in \mathbb{BDM}_h^{(1)}$ and p for the flux boundary condition (5.2b); the parameter δ is chosen as h^4.

DOFs	h	$\|\mathbf{u} - \mathbf{u}_h^{h^4}\|$	Rate	$\|\mathbf{u} - \mathbf{u}_h^{h^4}\|_{\text{div}}$	Rate	$\|p - p_h\|$	Rate
80	1/4	2.52166e−01	x	3.25377e+00	x	1.59554e−01	x
352	1/8	6.44209e−02	1.9688	1.63642e+00	0.9916	7.94309e−02	1.0063
1471	1/16	1.62002e−02	1.9915	8.19426e−01	0.9979	3.96269e−02	1.0032
6016	1/32	4.05619e−03	1.9978	4.09866e−01	0.9995	1.98008e−02	1.0009
24,320	1/64	1.01444e−03	1.9994	2.04952e−01	0.9999	9.89878e−03	1.0002

TABLE 5 Local mass conservation error in maximum norm as a function of δ for a fixed fine mesh size at $h = 1/64$.

δ	$\|\nabla \cdot \mathbf{u}_h - Q_h f\|_{\infty,T_h}$
1.e−03	0.78834D-05
1.e−04	0.78836D-06
1.e−05	0.78836D-07
1.e−06	0.78836D-08
1.e−07	0.78836D-09

We note that when we control the δ so that it gradually decreases to zero, Table 5 verifies the decay of local conservation error.

5.2 | The case of partial elliptic regularity

We next consider the L-shape domain problem with a constant coefficient in the non-convex domain $\Omega = (-1,1)^2 \setminus [0,1) \times (0,-1]$ with nonhomogeneous pressure boundary data g as given in (5.2a). As an exact solution, the harmonic function $p(r,\theta) = r^\alpha \sin(\alpha\theta)$ is taken, where $\alpha = \frac{2}{3}$ so that $p \in H^{\frac{5}{3}}(\Omega)$ and $g \in H^{\frac{7}{6}}(\Gamma)$.

We approximate $\mathbf{u}_h \in \mathbb{RT}_h^{(0)}$ and $\mathbf{u}_h \in \mathbb{BDM}_h^{(1)}$ on uniform meshes. For the choices of δ, we attempted to use $\delta = 1$ and $h^{\frac{4}{3}}$ on $\mathbb{RT}_h^{(0)}$, and $h^{\frac{10}{3}}$ on $\mathbb{BDM}_h^{(1)}$. We provide two results in Table 6, the computation of the flux variable, obtained with $\delta = 1$ and $\delta = h^{\frac{4}{3}}$ on $\mathbb{RT}_h^{(0)}$. In Table 7, the computation of the flux variable, obtained with $\delta = 1$ and $h^{\frac{4}{3}}$, is shown with the flux boundary condition (5.2b). In Table 8, the computation of the flux variable on $\mathbb{BDM}_h^{(1)}$, obtained with $h^{\frac{10}{3}}$, is shown for the pressure (5.2a) and the flux boundary condition (5.2b). The numerical results confirm that proper choices of parameter δ are important in using the Algorithm 2.

5.3 | The case of varying permeability tensor

It is well known that for the heterogeneous permeability tensor, the numerical solution often fails to converge due to the huge condition number. To overcome such a difficulty, several efficient preconditioners for $H(\text{div})$-bilinear form equation are proposed [3, 4, 16, 18, 19, 22]. For numerical example in this subsection, the $H(\text{div})$-preconditioner designed in [3] was implemented. The exact solution is the same as that of full ellipticity regularity case. The source function and boundary conditions are

TABLE 6 Errors and their reduction ratios of $\mathbf{u}_h \in \mathbb{RT}_h^{(0)}$ for the L-shape domain with pressure boundary condition (5.2a).

DOFs	h	$\|\mathbf{u}-\mathbf{u}_h^1\|$	Rate	$\|\mathbf{u}-\mathbf{u}_h^{\frac{4}{3}}\|$	Rate
44	1/4	2.90157e−01	x	2.77970e−01	x
160	1/8	2.05193e−01	0.4999	1.86047e−01	0.5793
608	1/16	1.44885e−01	0.5021	1.20496e−01	0.6267
2368	1/32	1.08681e−01	0.4148	7.70649e−02	0.6448
9344	1/64	8.94803e−02	0.2805	4.89770e−02	0.6540
37,120	1/128	8.03837e−02	0.1547	3.10161e−02	0.6591
147,968	1/256	7.64213e−02	0.0729	1.96008e−02	0.6621

Note: The parameter δ is chosen as 1 and $h^{\frac{4}{3}}$.

TABLE 7 Errors and their reduction ratios of $\mathbf{u}_h \in \mathbb{RT}_h^{(0)}$ for the L-shape domain with the flux boundary condition (5.2b).

DOFs	h	$\|\mathbf{u}-\mathbf{u}_h^1\|$	Rate	$\|\mathbf{u}-\mathbf{u}_h^{\frac{4}{3}}\|$	Rate
28	1/4	3.30758e−01	x	2.81957e−01	x
128	1/8	2.71112e−01	0.2869	1.93947e−01	0.5398
544	1/16	2.31156e−01	0.2300	1.29180e−01	0.5863
2240	1/32	2.08484e−01	0.1489	8.47662e−02	0.6078
9088	1/64	1.96699e−01	0.0839	5.51806e−02	0.6193
36,608	1/128	1.90804e−01	0.0439	3.57533e−02	0.6261
146,944	1/256	1.87865e−01	0.0224	2.30971e−02	0.6304

Note: The parameter δ is chosen as 1 and $h^{\frac{4}{3}}$.

TABLE 8 Errors and their reduction ratios of $\mathbf{u}_h \in \mathbb{BDM}_h^{(1)}$ for the L-shape domain with the pressure (5.2a) and the flux boundary condition (5.2b) with corresponding DOFs.

		BC (5.2a)		BC (5.2b)	
DOFs	h	$\|\mathbf{u}-\mathbf{u}_h^{\frac{10}{3}}\|$	Rate	$\|\mathbf{u}-\mathbf{u}_h^{\frac{10}{3}}\|$	Rate
88/56	1/4	1.18933e−01	x	1.24663e−01	x
320/256	1/8	7.51826e−02	0.6617	7.99052e−02	0.6417
1216/1088	1/16	4.74130e−02	0.6651	5.12513e−02	0.6407
4736/4480	1/32	2.98797e−02	0.6661	3.28582e−02	0.6413
18,688/18,176	1/64	1.88257e−02	0.6665	2.10542e−02	0.6421
74,240/73,216	1/128	1.18605e−02	0.6665	1.34834e−02	0.6429

Note: The parameter δ is chosen as $h^{\frac{10}{3}}$.

changed according to the exact solution and varying permeability field

$$\mathbb{A} = \begin{bmatrix} (x+2)^2+y^2 & \sin(\pi xy) \\ \sin(\pi xy) & 1 \end{bmatrix}. \tag{5.3}$$

With the use of V-cycle multigrid preconditioner, the numerical solution converges within a few iterations. Table 9 shows errors in the computation of the flux variable applying the hybrid method with

TABLE 9 Errors and their reduction ratios of $\mathbf{u}_h \in \mathbb{RT}_h^{(0)}$ for the varying permeability tensor with flux boundary condition.

DOFs	h	$\|\mathbf{u}-\mathbf{u}_h\|$	Rate	$\|\mathbf{u}-\mathbf{u}_h\|_{\text{div}}$	Rate
40	1/4	4.89318e+00	x	1.45608e+01	x
176	1/8	2.44908e+00	0.9985	7.37602e+00	0.9812
736	1/16	1.22496e+00	0.9995	3.69997e+00	0.9953
3008	1/32	6.12536e−01	0.9999	1.85148e+00	0.9988
12,160	1/64	3.06275e−01	1.0000	9.25928e−01	0.9997
48,896	1/128	1.53139e−01	1.0000	4.62987e−01	0.9999

Note: The parameter δ is chosen as h^2.

flux boundary condition (5.2b) and gives optimal convergence rates in the approximation of the flux variable with varying permeability tensor.

5.4 | The case of heterogeneous permeability tensor

We consider the following Darcy's flow problem with two-dimensional heterogeneous permeability tensor that is provided from the SPE10 Model 1. The domain is $\Omega = (0,100) \times (0, 20)$ and nonhomogeneous pressure boundary data $p_{\text{in}} = 1000$ and $p_{\text{out}} = 10$ are set on the left and right boundaries, respectively. The zero flux boundary conditions are imposed on the top and bottom boundaries. The source function in (5.1b) is set to be zero. For this example, uniform triangulations of Ω are adopted in our numerical simulation and the $\mathbb{RT}_h^{(0)}$ space is employed for the approximation of the flux variable. For the recovery of pressure, the $C^{-1}(P_h^{(0)})$ space is employed. For the comparison of our numerical results, the standard mixed finite element method space $\mathbb{RT}_h^{(0)} \times C^{-1}(P_h^{(0)})$ is employed to create reference numerical solutions. The values of heterogeneous permeability tensor are shown in Figure 1 with log scale. A figure for the (u, v) velocity fields and the recovered pressure field p by Algorithms 2 and 3 is also shown in Figure 2. We checked that the numerical results agree well with those by the standard mixed finite element approximation, and thus we omit the results for the latter. For the hybrid method, the computational mesh size h is chosen to be 0.5 and its corresponding optimal choice of the parameter δ is set to 2.5×10^{-5}. Since the flow drives in the negative direction of pressure gradient and pressure boundary condition is imposed on the inlet/outlet with specified values, the velocity in x-direction varies more widely comparing to the velocity in y-direction. The pressure field changes almost linearly with small variations in x direction.

Table 10 reports the CPU time comparison between the mixed finite element method and Algorithms 2 and 3 for the SPE10 data. For the time in assembling matrix, time for constructing stiffness matrix is necessary for the mixed finite element method, but in the case of the hybrid simple method, construction of mass and divergence matrices are needed additionally. However, for the resulting matrix system in the mixed finite element method, we need to solve positive indefinite system for velocity and pressure simultaneously. On the other hand, for the simple hybrid method, it is enough to solve positive symmetric definite system for the velocity and recover pressure separately. Overall computational time for solving flux and pressure variables by using the same direct linear solver or iterative minimum residual method (MINRES) [30] shows simple hybrid scheme is more efficient in computational time.

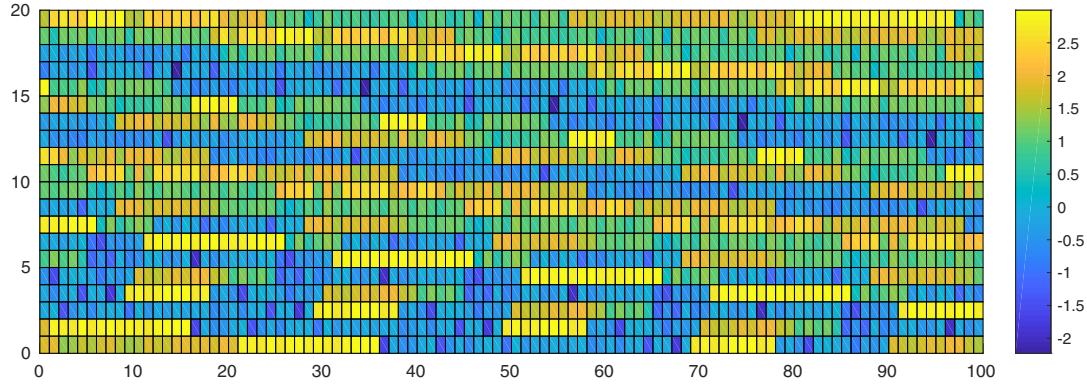

FIGURE 1 Permeability tensor with log scale from SPE10 model 1.

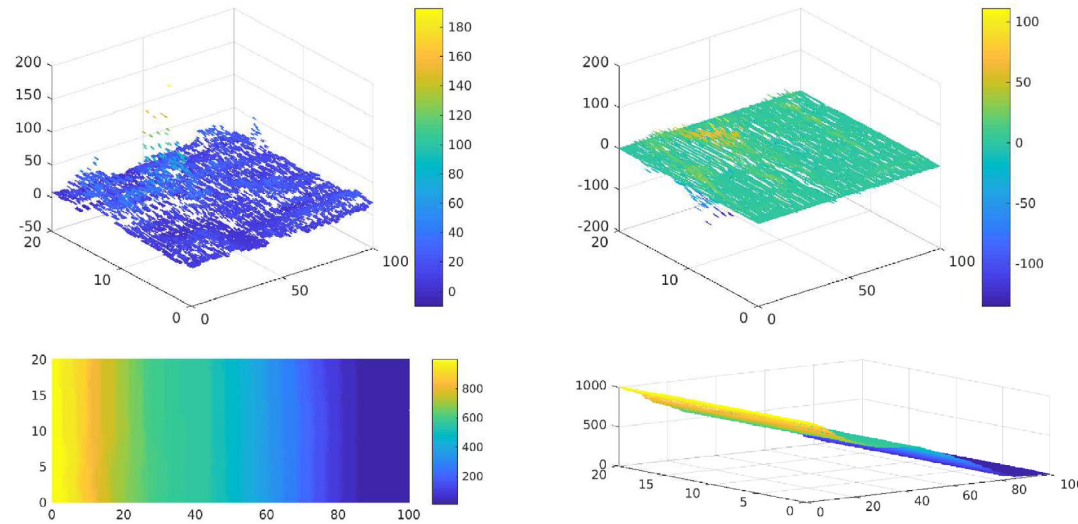

FIGURE 2 The velocity field (u, v) (upper) in $\mathbb{RT}_h^{(0)}$ by Algorithm 2 and the recovered pressure p (lower) in $C^{-1}(P_h^{(0)})$ by Algorithm 3 for SPE10 Model 1.

TABLE 10 The CPU time comparison of the standard mixed finite element method and our Algorithm 2.

	Assembling matrix	Direct solver	MINRES
Mixed method	1.3 s	5.9 s	340 s
Hybrid method	1.5 s	0.5 s	130 s

5.5 | The case of heterogeneous permeability tensor-SPE10 layer75

We consider the following Darcy's flow problem with two-dimensional heterogeneous permeability tensor that is provided from SPE10 Model 2 Layer75. The model dimensions are $1200 \times 2200 \times 170$ (ft) and the fine scale cell size is $20 \times 10 \times 2$ (ft) thus the domain is $60 \times 220 \times 85$. We only consider the single layer 75, the computational domain is $\Omega = (0, 60) \times (0,220)$. The zero flux boundary conditions are imposed on the top and bottom boundaries. For the left and right boundaries, nonhomogeneous pressure boundary data $p_{\text{in}} = 100{,}000$ and $p_{\text{out}} = 10$ is implied and the source function in (5.1b) is set

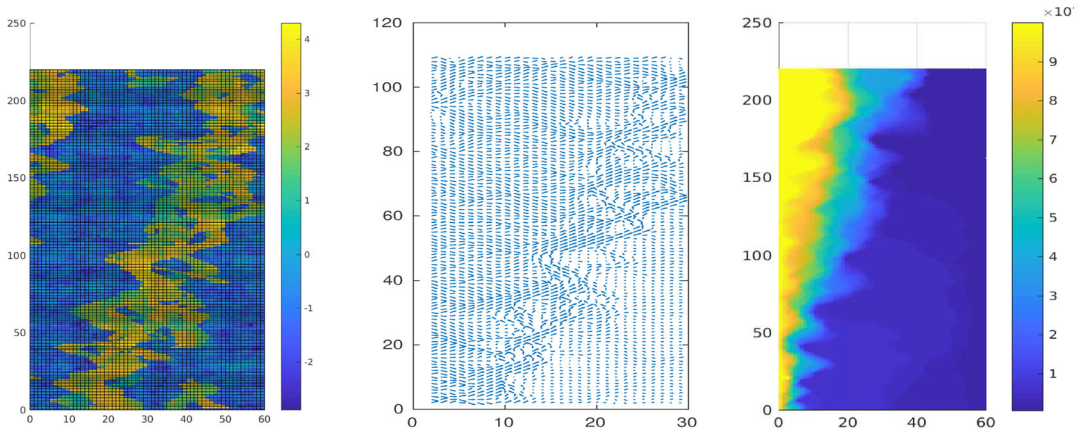

FIGURE 3 The permeability (left) for SPE Layer 75, the velocity field (u, v) (middle) in $\mathbb{RT}_h^{(0)}$ by Algorithm 2 and the recovered pressure p (right) in $C^{-1}(P_h^{(0)})$ by Algorithm 3 with specified pressure data on left/right and zero flux data on top/bottom boundaries.

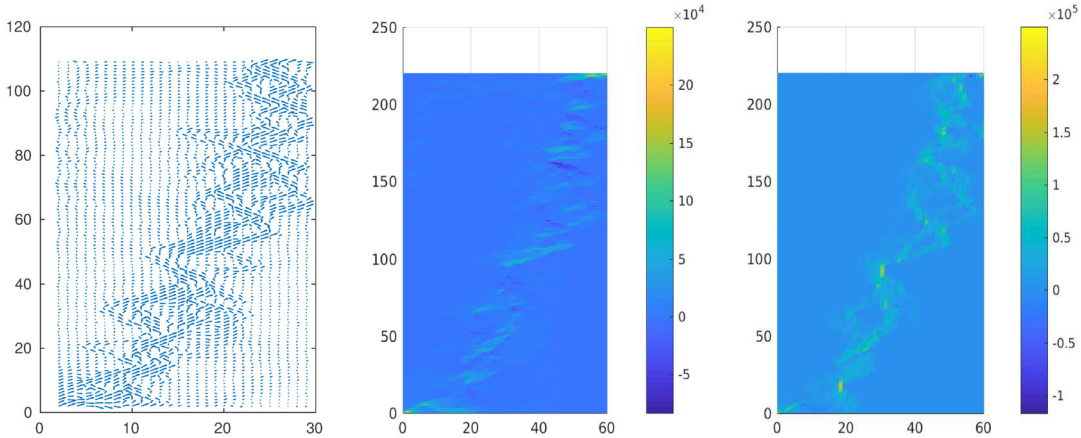

FIGURE 4 The (u, v) velocity quiver plot (left), u-(middle) and v-(right) fields with lowerleft point source and upperright point sink by Algorithm 2 using $\mathbb{RT}_h^{(0)}$.

to be zero. The values of heterogeneous permeability tensor are shown in the leftmost of Figure 3 with log scale. A flow plot for the (u, v) velocity field and the recovered pressure field p by Algorithms 2 and 3 are also shown in Figure 3. The plotted flow is averaged over eight triangles for the visibility. In the presence of point source at the leftlower and point sink at right upper corners with all zero flux boundary conditions, the numerical simulations are also performed and their results are shown in Figure 4. In this simulation, we can clearly see the flow pattern as we expected.

ACKNOWLEDGMENTS

The research of R. B. Adhikari was supported by NSF-DMS 2208289, and that of Y. J. Lee was supported by NSF-DMS 1318465 and DMS 2208499, while that of D. Sheen in part by National Research Foundation of Korea (NRF-2017R1A2B3012506 and NRF-2015M3C4A7065662).

CONFLICT OF INTEREST STATEMENT

The authors do not have any conflict of interest.

DATA AVAILABILITY STATEMENT

Data sharing not applicable—no new data generated, or the article describes entirely theoretical research.

ORCID

Dongwoo Sheen https://orcid.org/0000-0001-6857-7883

REFERENCES

[1] S. Agmon, *Lectures on elliptic boundary value problems*, Van Nostrand, Princeton, NJ, 1965.
[2] D. N. Arnold, *Finite element exterior calculus*, SIAM, Philadelphia, PA, 2018.
[3] D. N. Arnold, R. S. Falk, and R. Winther, *Preconditioning in H(div) and applications*, Math. Comput. 66 (1997), no. 219, 957–984.
[4] D. N. Arnold, R. S. Falk, and R. Winther, *Multigrid in H(div) and H(curl)*, Numer. Math. 85 (2000), no. 2, 197–217.
[5] D. N. Arnold, R. S. Falk, and R. Winther, *Finite element exterior calculus: From hodge theory to numerical stability*, Bull. Am. Math. Soc. 47 (2010), no. 2, 281–354.
[6] C. Bacuta, J. H. Bramble, and J. E. Pasciak, *Using finite element tools in proving shift theorems for elliptic boundary value problems*, Numer. Linear Algebra Appl. 10 (2003), no. 1-2, 33–64.
[7] D. Boffi, F. Brezzi, and M. Fortin, *Mixed finite element methods and applications*, Vol 44, Springer, Berlin, 2013.
[8] A. Bossavit, *"Mixed" systems of algebraic equations in computational electromagnetism*, COMPEL Int. J. Comput. Math. Electr. Electron. Eng. 17 (1998), 59–63.
[9] S. C. Brenner and L. R. Scott, *The mathematical theory of finite element methods*, Vol 3, Springer, Berlin, 2008.
[10] F. Brezzi, J. Douglas Jr., R. Durán, and M. Fortin, *Mixed finite elements for second order elliptic problems in three variables*, Numer. Math. 51 (1987), no. 2, 237–250.
[11] F. Brezzi, J. Douglas Jr., and L. D. Marini, *Two families of mixed finite elements for second order elliptic problems*, Numer. Math. 47 (1985), no. 2, 217–235.
[12] E. Di Nezza, G. Palatucci, and E. Valdinoci, *Hitchhiker's guide to the fractional Sobolev spaces*, Bull. Sci. Math. 136 (2012), no. 5, 521–573.
[13] J. Douglas Jr. and J. E. Roberts, *Global estimates for mixed methods for second order elliptic equations*, Math. Comput. 44 (1985), no. 169, 39–52.
[14] T. Gallouet and A. Monier, *On the regularity of solutions to elliptic equations*, Rend. Mat. Appl. VII 19 (1999), 471–474, 488.
[15] V. Girault and P. A. Raviart, *Finite element methods for Navier-Stokes equations: Theory and algorithms*, Vol 5, Springer Science & Business Media, Berlin, 2012.
[16] R. Hiptmair, *Multigrid method for H(div) in three dimensions*, Electron. Trans. Numer. Anal. 6 (1997), no. 1, 133–152.
[17] R. Hiptmair, *Finite elements in computational electromagnetism*, Acta Numer. 11 (2002), 237–339.
[18] R. Hiptmair and A. Toselli, "Overlapping and multilevel schwarz methods for vector valued elliptic problems in three dimensions," *Parallel solution of partial differential equations*, Springer, Berlin, 2000, pp. 181–208.
[19] R. Hiptmair and J. Xu, *Nodal auxiliary space preconditioning in H(curl) and H(div) spaces*, SIAM J. Numer. Anal. 45 (2007), no. 6, 2483–2509.
[20] J. Huang and Y. Xu, *Convergence and complexity of arbitrary order adaptive mixed element methods for the Poisson equation*, SCIENCE CHINA Math. 55 (2012), no. 5, 1083–1098.
[21] J. Jia, Y. J. Lee, and I. Ojeda-Ruiz, An efficient k-way constrained normalized cut and its connection to algebraic multigrid method, 2023.
[22] J. Kraus, R. Lazarov, M. Lymbery, S. Margenov, and L. Zikatanov, *Preconditioning heterogeneous H(div) problems by additive Schur complement approximation and applications*, SIAM J. Sci. Comput. 38 (2016), no. 2, A875–A898.
[23] J. Ku, *Supercloseness of the mixed finite element method for the primary function on unstructured meshes and its applications*, BIT Numer. Math. 54 (2014), no. 4, 1087–1097.
[24] J. Ku, Y. J. Lee, and D. Sheen, *A hybrid two-step finite element method for flux approximation: A priori estimates*, ESAIM Math. Model. Numer. Anal. 51 (2017), no. 4, 1303–1316.
[25] Y. J. Lee, J. Wu, J. Xu, and L. Zikatanov, *Robust subspace correction methods for nearly singular systems*, Math. Models Methods Appl. Sci. 17 (2007), no. 11, 1937–1963.

[26] M. Licht, *Smoothed projections and mixed boundary conditions*, Math. Comput. 88 (2019), no. 316, 607–635.
[27] J. C. Nédélec, *Mixed finite elements in* $\mathbb{R}^3$, Numer. Math. 35 (1980), 315–341.
[28] I. Ojeda-Ruiz and Y. J. Lee, *A fast constrained image segmentation algorithm*, Results Appl. Math. 8 (2020), 100103.
[29] P. A. Raviart and J. M. Thomas, "A mixed finite element method for 2nd order elliptic problems," *Mathematical aspects of finite element methods*, Springer, Berlin, 1977, pp. 292–315.
[30] Y. Saad, *Iterative methods for sparse linear systems*, SIAM, Philadelphia, PA, 2003.
[31] G. Savaré, *Regularity and perturbation results for mixed second order elliptic problems*, Commun. Partial Differ. Equ. 22 (1997), no. 5-6, 869–899.
[32] R. Stenberg, *Postprocessing schemes for some mixed finite elements*, ESAIM Math. Model. Numer. Anal. 25 (1991), no. 1, 151–167.

How to cite this article: R. B. Adhikari, I. Kim, Y. J. Lee, and D. Sheen, *An efficient flux-variable approximation scheme for Darcy's flow*, Numer. Methods Partial Differ. Eq. (2024), e23120. https://doi.org/10.1002/num.23120